THE JOURNAL OF PHYSICAL CHEMISTRY C

Article

pubs.acs.org/JPCC

Experimental Evidence and Modified Growth Model of Alloying in $In_xGa_{1-x}As$ Nanowires

R-Ribeiro Andrade,[†,*] A. Malachias,[†,‡] G. Kellerman,[‡] F. R. Negreiros,[†] N. M. Santos,[§] N. A. Sobolev,[§] M. V. B. Moreira,[†] A. G. de Oliveira,[†] and J. C. González[†]

[†]Departamento de Física, Instituto de Ciências Exatas, Universidade Federal de Minas Gerais, Postal Code 702, 30123-970, Belo Horizonte, Brazil.

[‡]Laboratório Nacional de Luz Síncrotron, C.P. 6192, 13083-970, Campinas, SP, Brazil

[§]I3N and Departamento de Física, Universidade de Aveiro, 3810-193 Aveiro, Portugal

ABSTRACT: In this work, a systematic study of the influence of growth conditions on the anomalous formation of ternary $In_xGa_{1-x}As$ nanowires is presented. Free-standing nanowires, of nominal InAs composition, were grown by molecular beam epitaxy on GaAs (111)B substrates at different temperatures and As_4 beam equivalent pressures. The morphology, chemical composition, and crystal structure of the nanowires were investigated by scanning electron microscopy, X-ray energy dispersive spectroscopy, and X-ray diffraction techniques. It was found that a strong incorporation of Ga occurs during the growth creating a homogeneous ternary $In_xGa_{1-x}As$ alloy in the nanowires with very low residual strain. The GaAs molar fraction was found to increase with the growth temperature and to decrease with the As_4 beam equivalent pressure. A nanowire growth model, taking into account the creation and diffusion of Ga adatoms from the substrate surface toward the nanowires, was used to explain the incorporation of Ga atoms and the formation of the ternary alloy. This model predicts that the GaAs/InAs composition ratio in the nanowires follows an Arrhenius law as a function of the growth temperature with an inverse square root dependency of the As_4 beam equivalent pressure as a pre-exponential factor. The theory was found to fit well the experimental data with an activation energy of 1 eV. It is also shown that the activation energy corresponds to the energy necessary to create Ga adatoms on the surface of the GaAs (111)B substrate. Both experimental and theoretical results show that in this range of growth conditions the limiting factor for the formation of the $In_xGa_{1-x}As$ alloy in the nanowires is not the diffusion length of the Ga and In adatoms on the substrate surface and nanowires side walls but the density of available Ga adatoms on the substrate surface.

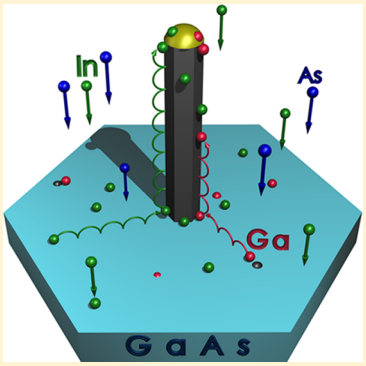

INTRODUCTION

III−V free-standing nanowires (NWs) have been intensively studied due to the inherent potential of these nanostructures for optoelectronic and sensor applications. Several research groups have reported a precise control of III−V NWs growth by a large variety of methods.[1−8] These studies have been also extended to ternary III−V NWs, usually grown in GaAs (111)B substrates, that allow band gap engineering for device applications.[10−12] However, the influence of the substrate and growth conditions in this heteroepitaxy has been barely studied. In a previous work,[4] we have shown, for a particular case, that Ga atoms from the substrate can be incorporated into the nanowires during growth. Here, it will be shown that parameters such as growth temperature (T_G) and group V beam equivalent pressure (BEP) strongly influence that incorporation, playing an important role in the modification of the structural and chemical properties of InGaAs free-standing NWs grown on GaAs (111)B substrates by molecular beam epitaxy (MBE).

Free-standing nanowires with nominal InAs composition were grown by MBE on GaAs (111)B substrates at several T_G and As_4 BEP. Scanning electron microscopy (SEM), X-ray energy dispersive spectroscopy (EDS), and X-ray diffraction in coplanar (XRD), and grazing incidence geometry (GID) were used to study the morphology, chemical composition, and crystal structure of the NWs, respectively. These studies have shown an anomalous incorporation of Ga in the NWs creating a homogeneous $In_xGa_{1-x}As$ ternary alloy with none or very low residual strain. The GaAs molar fraction in the ternary alloy was found to increases with T_G and to decreases with the As_4 BEP reaching values between 3% and 19%. To explain the incorporation of Ga in the NWs, a nanowire growth model accounting for the creation and diffusion of Ga adatoms from the GaAs substrate is introduced.

EXPERIMENTAL SECTION

The nanowires were grown by MBE (RIBER 2300 RD system) on GaAs (111)B substrates drop coated with colloidal gold nanoparticles, dispersed in water, of 5 nm in diameter. The growth procedure starts by removing the protective oxide layer from the substrate surface at 655 °C under As_4 flux during 20 min. The deoxidation process and quality of the surface of the

Received: May 23, 2012
Revised: October 24, 2012
Published: October 25, 2012

dx.doi.org/10.1021/jp305031h | J. Phys. Chem. C 2012, 116, 24777−24783

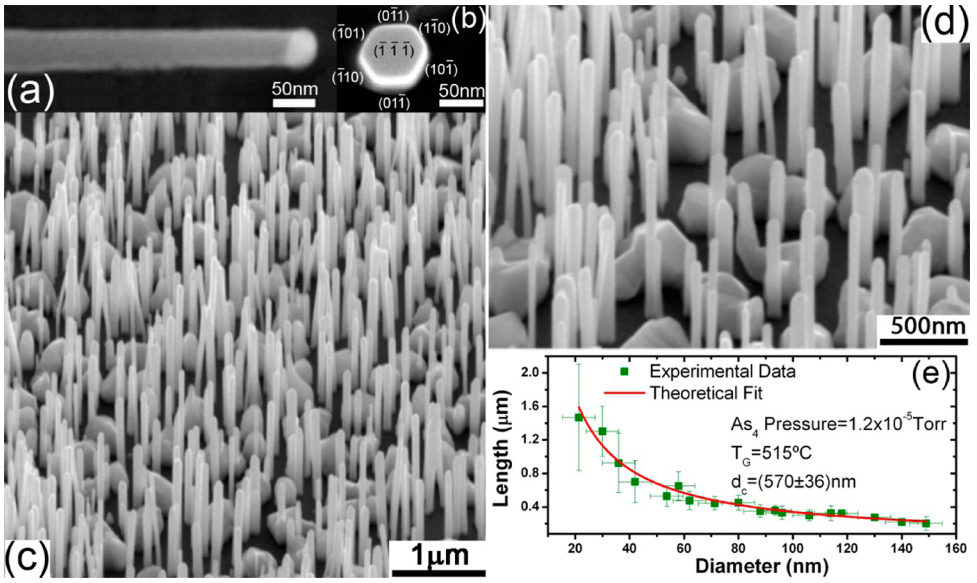

Figure 1. SEM images of the NWs. (a) side view of a NW showing the metal particle at the tip. (b) top view of a NW showing a hexagonal cross-section. (c) 30°-Perspective low magnification view of the NWs. (d) 30°-Perspective high magnification view showing the InAs grains formed in between the NWs, as well as clear substrate areas around the base of the NWs. (e) Length-diameter dependency of the NWs. The solid line in (e) is the fit of eq 1 to the experimental data.

substrate was confirmed by obtaining a high quality 2D reflection high energy electron diffraction (RHEED) patterns. After deoxidation, the substrate temperature was lowered to the growth value and the sample exposed to a flux of In atoms. The In BEP used during the growth was of 2.8×10^{-7} Torr for all the samples. The Ga evaporation cell of the MBE system was kept cold and close during the whole growth procedure. After 20 min of growth the flux of In atoms was interrupted and the sample was cooled down to room temperature under As_4 flux. Two sets of samples were grown in different conditions: (i) three samples grown with As_4 BEP of 1.2×10^{-5} Torr and T_G = 500 °C, 515 and 560 °C, (ii) three samples grown with As_4 BEP of 1.0×10^{-6} Torr and T_G = 485 °C, 515 and 530 °C.

SEM and EDS measurements were carried out in order to study the morphology and the chemical composition of the NWs. X-ray diffraction experiments were carried out at the XRD2 beamline of the Brazilian National Light Synchrotron Laboratory at 10.261KeV X-ray energy. This beamline is equipped with a 4 + 2-circle Huber diffractometer. Two different diffraction geometries were used. A noncoplanar geometry was initially used to perform grazing-incidence diffraction (GID) allowing the determination of the lattice parameter of the crystal planes of the nanowires perpendicular to the substrate surface (in-plane lattice parameter). In addition, coplanar diffraction was used to measure reflections that provide the lattice parameter along the wires axis (out-of-plane lattice parameter) and asymmetric reflections that combine in-plane and out-of-plane information.

RESULTS AND ANALYSIS

Figure 1 shows the typical morphology of the samples. The NWs, observed in parts a–d of Figure 1, exhibit the shape of hexagonal bars oriented perpendicular to the substrate surface along the $[\bar{1}\bar{1}\bar{1}]$ direction and bounded by six vertical $\{\bar{1}10\}$ facets. A metallic particle, of approximately the same diameter as the NWs (part a of Figure 1), can be seen at the tip of the NWs. Large grains are also visible on the surface of the substrate, in between the NWs (parts c and d of Figure 1). Part d of Figure 1 also shows that most of the NWs are surrounded by clear substrate areas, with no grains. Finally, part e of Figure 1 shows the length-diameter dependency L(d) of the NWs. The shape of this curve indicates that the diffusion of adatoms from the substrate surface increases the NWs growth rate.[13,14]

EDS elemental analyses of the NWs are presented in Figure 2. The electron beam energy was chosen to be 12 keV, high enough to excite the L lines of the elements of interest and to maximize the EDS signal-to-noise ratio. These analyses were carried out in NWs dispersed on a pirolitic carbon substrate to eliminate the influence of GaAs substrate on the EDS spectra and the EDS line scans of the NWs. As there are not appreciable excitation of atoms away from incidence point, the scan resolution is close to NW diameter and the spatial resolution of the EDS measurements is good enough to observe possible elements concentration gradients along the NWs. EDS resolution was confirmed by Monte Carlo simulations of X-ray emission performed with CASINO v. 2.48.[15] The EDS spectrum of a single NW is shown in part a of Figure 2. Strong peaks of In and As, as well as a small peak of Au can be seen in the spectrum. However, a surprisingly strong signal of Ga can be also observed. The EDS line scans of these elements, shown in part b of Figure 2, present a homogeneous distribution of In, Ga and As along the NW. Part c of Figure 2 shows the line scan analyzed NW. The homogeneous distribution of In, Ga and As in the NW indicates the formation of a ternary $In_xGa_{1-x}As$ alloy in the NWs during the growth of the samples. As observed in the NWs micrographs (part d of Figure 1), they present a constant diameter from their bottom to their apex. The only known process that produces NWs with constants diameter is diffusion-induced (DI) growth.[13,14] The DI growth mechanism was confirmed by the characteristic length-diameter dependency L(d) of the NWs.[13,14] It is also known that the radius of the catalyst particle is dependent on the precursors supersaturation[13,14] indicating that, at steady state, the supersaturation of the catalyst particle is also constant during the growth. These observations discard the possible incorporation of a large amount of Ga in the catalyst at the

dx.doi.org/10.1021/jp305031h | J. Phys. Chem. C 2012, 116, 24777–24783

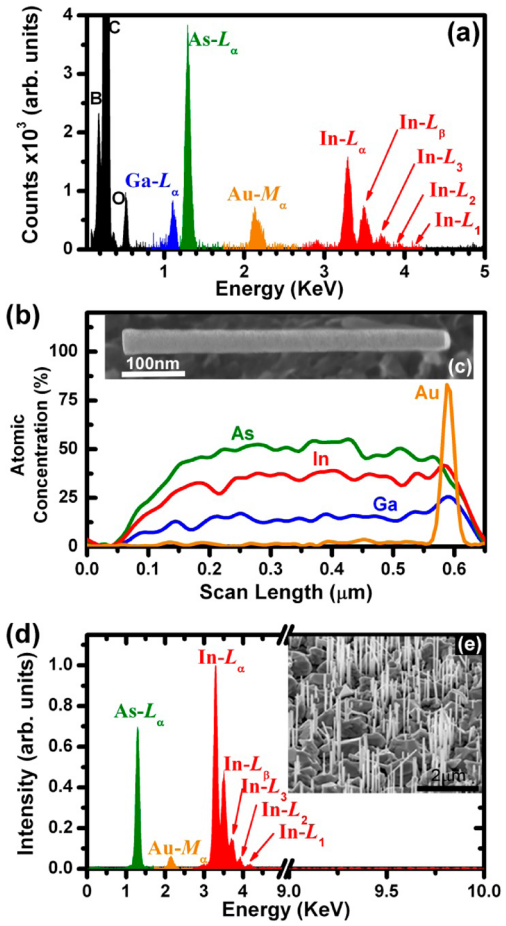

Figure 2. EDS elemental analysis of the NWs. (a) Typical EDS spectrum of individual NWs dispersed in pirolitic carbon denoting the presence of Au, In, As, and Ga. (b) EDS line scan of single NW (c) showing the homogeneous distribution of In, As, and Ga along the NW, whereas Au is concentrated at the tip of the NW. (d) Typical EDS spectrum of InAs NWs grown on InAs (111)B substrates, shown in the inserted image (e), denoting the presence of just In, Au, and As, and ruling out any possible residual Ga contamination in the chamber.

beginning of the growth since, it should be observed either tapered NWs or a richer in Ga composition at the NWs top. However, neither of these two possibilities was observed in SEM images and EDS experiments. The same experiments were carried out in several NWs of different lengths with similar results. The atomic concentration of Ga in the NWs was found to be in the range from 3% to 10% corresponding to a GaAs molar fraction between 6% and 20%, respectively. The EDS spectrum of a InAs NWs control sample grown on an InAs (111)B substrate is shown in part d of Figure 2. EDS peaks of Ga were not observed for that sample, as seen in part e of Figure 2, demonstrating that the Ga content in the NWs is not due to contamination of the growth chamber. An increase of the Ga content was observed, for the samples grown in GaAs (111)B substrates, as the growth temperature increases. However, because of the small volume of material in the NWs and the quantification errors induced by the geometry of the NWs, the elemental concentrations obtained from the EDS spectra are not accurate. Under these conditions, the error in the GaAs molar fraction was estimated in 5%. A more precise and statistically representative determination of the mean GaAs molar fraction in the NWs is retrieved by X-ray diffraction measurements, as discussed below.

X-ray diffraction experiments were carried out in coplanar and grazing incidence geometries. These experiments allow obtaining an accurate lattice parameter along several crystal directions, from which the strain and the GaAs molar fraction in the NWs can be extracted. Figure 3 shows radial (θ-2θ) scans along two GID and two coplanar reciprocal space directions in the vicinity of the $(2\bar{2}0)$, $(2\bar{4}2)$, $(00\bar{2})$ and $(\bar{3}\bar{3}\bar{3})$ reflections, respectively. The $(2\bar{2}0)$ and $(2\bar{4}2)$ radial scans probe the in-plane lattice parameter distribution inside the NWs along two nonparallel directions. The $(\bar{3}\bar{3}\bar{3})$ scan probes the out-of-plane lattice parameter distribution along the growth direction of the NWs. Finally, the scan in the vicinity of the asymmetric $(00\bar{2})$ reflection probes a combination of in-plane and out-of-plane lattice parameters. The horizontal axis of all diffractograms shown in Figure 3 are in radial momentum transfer $Q_r = (4\pi/\lambda)\sin(2\theta/2)$ scale. A representation of the relative orientation of the NWs with respect to the substrate as well as the directions of the scattering vectors is shown in part a of Figure 3. Two strong diffraction peaks are observed in the diffractograms corresponding to the bulk GaAs and InAs lattice parameters of 5.653 and 6.058 Å respectively,[16] whereas a shoulder can be observed at the right side of the InAs peak. In addition to the shoulder, a slight asymmetry can be also observed at the left side of the InAs peak. This asymmetry could be attributed to the diffraction from a volume of wurtzite phase in the NWs. However, the wurtzite volume is considerably reduced with respect to the zinc blende volume found in the NWs and it will be considered negligible for this study of the impact of the Ga adatoms diffusion on the zinc blende phase. The GaAs and InAs peaks have been identify as the diffraction from the GaAs substrate and the InAs grains formed in between the NWs.[4] The shoulder, due to the diffraction from a structure with a lattice parameter smaller than that of bulk InAs, was identified as corresponding to the NWs (for a detailed discussion, ref 4). The local lattice parameter obtained from the position of the shoulder was found to be the same for the four reflections demonstrating that the NWs present a crystal structure with cubic symmetry with a very low residual strain. This cubic crystal structure with a lattice parameter lower than that of bulk InAs indicates the formation of a homogeneous $In_xGa_{1-x}As$ alloy in the NWs, in agreement with the EDS observations. The GaAs molar fraction $(1 - x)$ in the NWs can be obtained from the comparison of the NWs lattice parameter with the Vergaás law prediction for bulk $In_xGa_{1-x}As$.[16] For that purpose were used the $(2\bar{2}0)$ diffractograms of the samples as shown in Figure 4. In these graphs, the radial momentum transfer Q_r axis was converted to local lattice parameter to allow a direct comparison of the measurements. A systematic shift of the shoulder lattice parameter toward lower values is observed as the growth temperature increases and the As_4 BEP decreases. Such a reduction of the NWs lattice parameter indicates a Ga enrichment of the $In_xGa_{1-x}As$ alloy at higher temperatures and lower As_4 BEP as shown in Figure 5.

GROWTH MECHANISM AND ALLOYING

The formation of $In_xGa_{1-x}As$ alloys during the growth of NWs with InAs nominal composition should be explained by taking into consideration the MBE growth process of the NWs. The most reported growth mechanism of NWs is the so-called Vapor−Liquid−Solid (VLS) growth,[17,18] where the growth is produced by the direct impingement of primary molecular

dx.doi.org/10.1021/jp305031h | J. Phys. Chem. C 2012, 116, 24777−24783

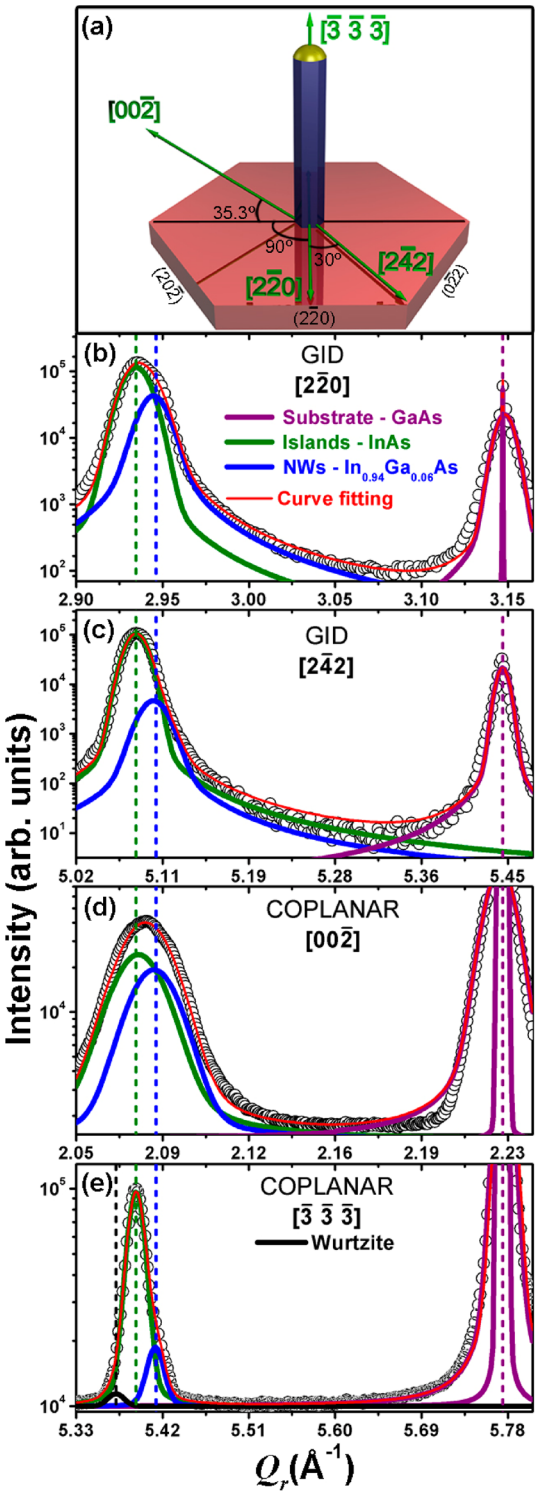

Figure 3. Radial scans of the (2$\bar{2}$0), (24$\bar{2}$), (00$\bar{2}$), and ($\bar{3}\bar{3}\bar{3}$) reflections of the NWs sample grown at 515 °C. Note the shoulder observed at the right side of the InAs peak. In (a) the relative orientation of the NW with respect to the substrate and the directions of the scattering vectors are represented. The solid lines are the best fits of Voigt functions to the experimental data. In (e) the black curve correspond to (0006) wurtzite. The small area of the (0006) wurtzite curve indicates the reduced volume of wurtzite in our nanowires.

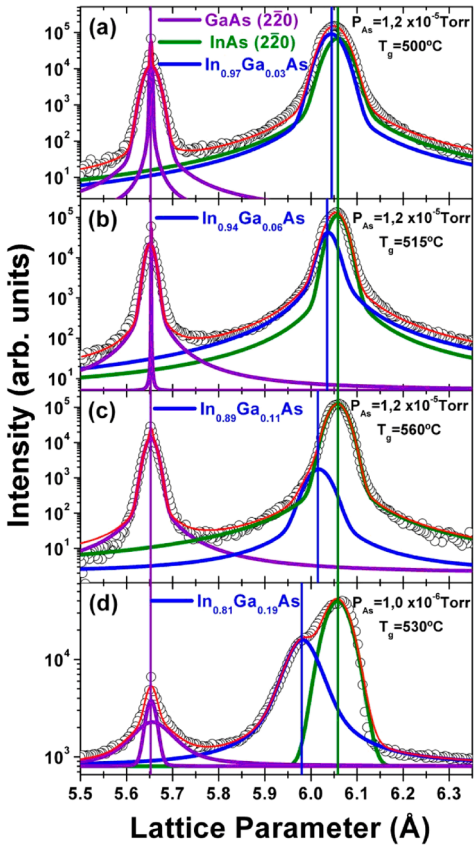

Figure 4. X-ray radial ($\theta - 2\theta$) scans near the (2$\bar{2}$0) reflection of samples grown at different T_G and As_4 BEP. Note the shift toward lower lattice parameter of the shoulder at the left side of the InAs peak as T_G increases and As_4 BEP decreases. The solid lines are the best fit of Voigt functions to the experimental data.

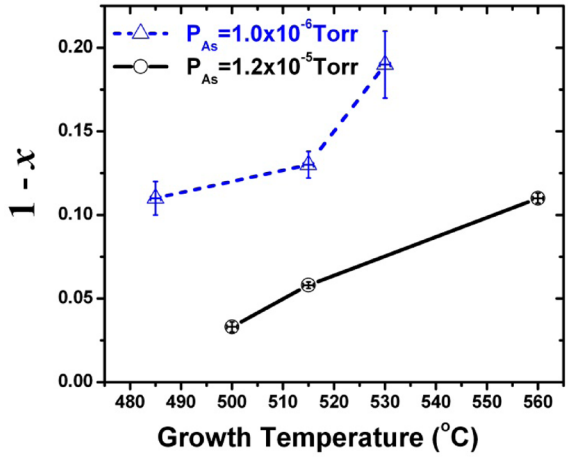

Figure 5. Temperature dependence of the mean GaAs molar fraction in NWs for the low and high As_4 BEP series of samples.

beams, that is thermally evaporated In atoms and As_4 molecules, at the surface of the liquid catalyst at the top of the NWs. It has been shown that in some cases the growth of III−V NWs does not satisfy all of the conditions for the VLS model because at low growth temperatures the catalyst will not be in a liquid state.[19] However, the growth temperature of the samples studied here is sufficiently higher than the eutectic temperatures of the Au−In (454 °C), Au−Ga (334 °C), and Au−Ga−In (≤300 °C for ~$Au_{0.63}Ga_{0.11}In_{0.26}$) systems[20] to ensure that the catalyst at the top of the NWs is in liquid state during the growth. However, the VLS growth model alone cannot explain the anomalous incorporation of Ga in the NWs.

dx.doi.org/10.1021/jp305031h | J. Phys. Chem. C 2012, 116, 24777−24783

Furthermore, under certain growth conditions it has been demonstrated that the NWs growth can be induced by the surface diffusion toward the NW base of a fraction of the primary molecular beams, that is the incoming In atoms, impinging regions of the substrate in between the NWs.[13,14] This so-called diffusion-induced (DI) growth mechanism generalizes the VLS mechanism for free-standing NWs grown on epitaxial substrates under conditions of strong surface diffusion. Experimentally, it is simple to determine the dominant growth mechanism of the NWs by measuring their $L(d)$ dependency: a dominant VLS growth exhibits an increasing $L(d)$ curve,[17,18] whereas a dominant DI growth exhibits a decreasing $L(d)$ curve of the form:[13,14]

$$L(d) = \left(V + \frac{d_c}{d}\right)H \tag{1}$$

where V is the contribution to the length of the NWs due to the absorption and desorption of precursors in the catalyst drop, H is the equivalent thickness of the film growing in between the NWs, d is the diameter of the NWs and d_c is a critical diameter. For NWs thicker than the critical diameter the VLS mechanism is dominant over the DI growth mechanism. As shown in part e of Figure 1, the growth of our NWs is clearly dominated by the DI mechanism.

The DI growth mechanism, as above explained, can take into account the incorporation of Ga into the NWs if an additional source supplies this precursor during the growth. The additional Ga sources could be due, in our case, to: (i) reevaporation of Ga contamination in the growth chamber, (ii) residual evaporation from the close and cold Ga cell of the MBE system, (iii) diffusion of a thermally created population of Ga adatoms on the GaAs substrate surface. The two first sources should equally contribute to all the samples grown in the same MBE system under similar conditions. However, as shown in part d of Figure 2, the presence of Ga was not observed in the InAs NWs control sample grown on a InAs (111)B substrate discarding the firsts two possibilities. Therefore, the Ga content in the NWs grown on GaAs (111) B substrate is due to the diffusion of thermally created Ga adatoms from the substrate surface toward the NWs tip. This mechanism of Ga incorporation can occur in the NWs as well in the islands. However, the GID diffractrograms show no evidence of Ga incorporation in the islands. It is important to stress that islands are incoherent (relaxed) deposits without clear faceting. The fact that these deposits are relaxed makes them preferential sites for InAs nucleation. The absence of clear facets does not allow for the large surface mobility observed in the wires, hence limiting the gallium adatoms interdiffusion from the substrate surface to the islands. SEM observations also show that the islands present much larger volumes than the NWs. Therefore, even if a small amount of gallium adatoms incorporates into the islands − considering a scenario where incorporation of adatoms scales with the perimeter of the each kind of nanostructure − the GaAs molar fraction in the islands would be much lower than in the NWs and very difficult to detect by EDS or XRD. Therefore, within the chemical sensitivity of EDS and XRD, the islands can be considered as made of InAs. In fact, the X-ray experiments do not detected appreciable changes in the islands lattice parameter.

The contribution of Ga adatoms to NWs follows the DI mechanism. Therefore, the steady-state growth rate of the NWs can be expressed as $R_{NW} = R_0 + R_{diff}^{In} + R_{diff}^{Ga}$, where R_0 is the growth rate due to the direct impingement of In atoms on the top of the NW and R_{diff}^{In} and R_{diff}^{Ga} are the contributions to the growth rate due to the diffusion flux of In and Ga surface adatoms, respectively. In the diffusion-induced regime, the R_0 contribution can be neglected for thin NWs with diameters smaller than critical diameter, with a minimum value of 140 nm for our samples. Therefore, the average InAs molar fraction x in the NWs can be approximated as:

$$x = \frac{R_{diff}^{In}}{R_{NW}} = \frac{R_{diff}^{In}}{R_{diff}^{In} + R_{diff}^{Ga}} \tag{2}$$

Both In and Ga diffusion growth rates are proportional to the diffusion flux of In and Ga adatoms from the substrate surface to the top of the NWs. Following Dubrovskii et al.,[13,14] the diffusion flux $j_{diff}(L)$ for each element can be expressed by:

$$j_{diff}(L) = j_{diff}(0)\frac{1}{\cosh(L/\lambda_f)} \tag{3}$$

where L is the length of the average NW, λ_f is the diffusion length of the adatom (Ga or In) on the {110} sidewalls of the InAs NWs, and $j_{diff}(0) = l_s \pi d \sigma N_{eq}/4t_s$ is the diffusion flux of surface adatoms reaching the NWs base. Here, l_s (∼ 4 Å for GaAs) is the length of adatom diffusion jump, d is the nanowire diameter, t_s is the characteristic time between jumps, σ (∼1 under typical MBE conditions[21,22]) is the adatom supersaturation on the substrate surface and N_{eq} is the equilibrium adatom concentration on the substrate surface. Therefore,

$$\frac{1}{x} - 1 = \frac{j_{diff}^{Ga}(0)}{j_{diff}^{In}(0)}\frac{\cosh(L/\lambda_f^{In})}{\cosh(L/\lambda_f^{Ga})} \propto \frac{N_{eq}^{Ga}}{N_{eq}^{In}} \tag{4}$$

Eq 4 shows that the ratio between the InAs and GaAs molar fraction in the NWs can be limited by the diffusion lengths of Ga and In adatoms as well as the equilibrium concentration of Ga and In adatoms. Under our experimental conditions the diffusion lengths λ_f of In and Ga adatoms are on the order of 5−10 μm,[23−26] much larger than the average NW length (∼1 μm) in our samples. Therefore, the evaluation of the hyperbolic cosines of eq 4 gives approximately unit, meaning that the diffusion lengths of adatoms are not a limiting factor for the incorporation of Ga in the NWs. This argument is also supported by the EDS and XRD experimental observation of a homogeneous distribution of Ga in the NWs. Furthermore, it has been observed that in a growth limited by the diffusion length of the adatoms the NWs exhibit a tapered morphology with a neck below the catalytic particle of a length equal to the surface diffusion length of the adatoms.[20,27] The NWs discussed here are straight hexagonal bars (Figure 1) with not evident tapering. Hence, the growth is not limited by the diffusion length of the adatoms and the diffusion term in eq 4 can be reduced to the ratio between the equilibrium concentration of In and Ga adatoms on the surface of the substrate. This result implies that the ability of the substrate surface to supply Ga adatoms should be the limiting growth factor for the alloying in the NWs. Therefore, the available amount of Ga in the collection area of the NWs on the surface of the substrate should be larger than the amount of Ga experimentally found in the NWs. Considering the atomic areal density of the first monolayer of Ga on the surface of a 2 × 2 reconstructed GaAs (111)B substrate as 3×10^{14} cm^{-2}, the diameter of the adatom collection area of the average NW as the average distance between the NWs, and the average volume of the NWs for each

dx.doi.org/10.1021/jp305031h | J. Phys. Chem. C 2012, 116, 24777−24783

sample, we have estimated that the NWs consume approximately 30% or less of the available amount of Ga in the substrate surface.

Neglecting variations of the desorption of In adatoms in the growth temperature range of our samples,[28] the equilibrium concentration of In adatoms should be approximately constant and independent of the growth temperature. However, the equilibrium concentration of Ga adatoms strongly depends on the temperature of the substrate and the As_4 BEP (P_{As}).[29] Therefore, the temperature and As pressure dependence of the average GaAs/InAs composition ratio in the NWs can now be expressed as:

$$\frac{1}{x} - 1 \propto \frac{1}{N_{eq}^{In}\sqrt{P_{As}}} e^{-E_a/kT_G} \quad (5)$$

where k is the Boltzmann constant and E_a is the energy necessary for the creation of a Ga adatoms.

Figure 6 shows an Arrhenius plot of the growth temperature dependence of the $(P_{As})^{1/2}(1/x - 1)$ for the two sets of NWs

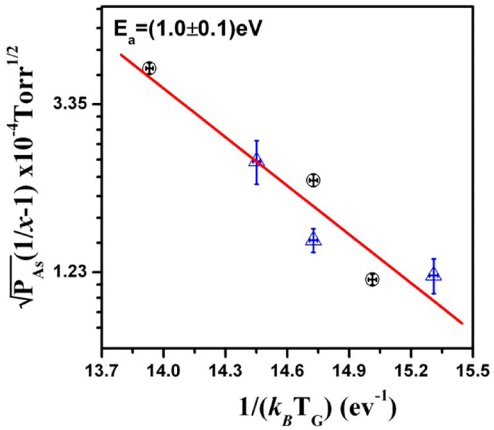

Figure 6. Growth temperature dependence of the Ga incorporation in the NWs. The solid line is the best fit of eq 5 to the experimental data, with slope indicated by E_a.

samples grown under different As_4 BEP. The data in Figure 6 exibit only one activation energy of (1.0 ± 0.1) eV. These results are in agreement with eq 5 and show that only one process dominates the incorporation of Ga in the NWs in the interval of growth conditions investigated here. To further corroborate the validity of the above presented growth model the energy necessary to create Ga adatoms on a 2 × 2 reconstructed GaAs (111)B surface should be similar to the value of the activation energy obtained from the experimental data. This energy can be calculated as $E_x = B_{GaAs} - B_{Ga} - B_{As}$,[29] where B_{GaAs} = 6.8 eV[30] is the cohesive energy of GaAs per two atoms, B_{Ga} is the binding energy of a free Ga atom to the surface, and B_{As} = 2.7 eV[30] is the cohesive energy per atom of an As_4 molecule. The unknown value of B_{Ga} can be calculated by ab initio DFT simulations. We have performed these calculations with the plane-wave-based Quantum Espresso package[31,32] that solves the Kohn−Sham equations using the generalized-gradient exchange-correlation functional approximation proposed by Perdew, Burke, and Ernzerhof[31] Spin polarized calculations were carried out with an energy cutoff of 340 eV ensuring an accurate determination of both the bulk equilibrium properties of Ga and As and the energies of these atoms when completely isolated. The reconstructed GaAs(111)B-2 × 2 surface was modeled using an asymmetric slab composed of 5 layers each with 16 Ga or As atoms plus a surface layer with 8 As atoms. During the simulation, the last two layers and the removed Ga adatom were kept fixed and the positions of all the other atoms were optimized without any constraint until forces on each atom were less than 0.03 eV/Å. The distance between the Ga adatom and the surface was increased by approximately 0.07 Å in each step. The vacuum region separating neighbor slabs was equal to 14 Å, what guaranteed a distance of 7 Å between the completely removed Ga adatom and the consecutive slab. For this unit cell, the Brillouin-zone integration was performed using a Monkhorst-Pack k point sampling with a 4 × 4 × 1 k-point mesh. From this simulation a value of B_{Ga} = 2.8 eV was obtained, which gives E_x = 1.3 eV. Kaxiras et al.[30,33] have reported similar calculations with values of B_{Ga} between 2.99 and 3.31 eV. Therefore, values of E_x between 0.8 and 1.1 eV can be derived from such calculations. These results show that the value of the energy necessary to create Ga adatoms on the reconstructed GaAs(111)B-2 × 2 surface is in agreement with the activation energy found in the experiments.

CONCLUSIONS

In this work, we have studied the influence of parameters such as growth temperature and As_4 BEP on the morphology, chemical composition and crystal structure of free-standing nanowires with nominal InAs composition and grown by MBE. We have shown that the NWs suffer a strong thermally activated incorporation of Ga, that creates a homogeneous $In_xGa_{1-x}As$ alloy in the NWs with none or very low residual strain. The GaAs molar fraction in the ternary alloy was found to increases with T_G and to decreases with the As_4 BEP, reaching values between 3% and 19%. The incorporation of Ga in the NWs is due to the temperature activation of a large population of Ga adatoms on the surface of the GaAs (111)B substrate that diffuse toward the NWs. A generalization of the DI growth model was used to explain our experimental results taking into account the creation of Ga adatoms on the substrate surface as well as the diffusion of these toward the NWs. This model predicts that the GaAs/InAs composition ratio in the nanowires follows an Arrhenius law as a function of the growth temperature, with an inverse square root dependency of the As_4 beam equivalent pressure as a pre-exponential factor. The theory was found to fit well the experimental data with an activation energy of 1 eV. It is also shown that the activation energy corresponds to the energy necessary to create Ga adatoms on the surface of the GaAs (111)B substrate. Both experimental and theoretical results show that in this range of growth conditions the limiting factor for the formation of the $In_xGa_{1-x}As$ alloy in the nanowires is not the diffusion length of the Ga and In adatoms on the substrate surface and nanowires side walls but the density of available Ga adatoms on the substrate surface.

AUTHOR INFORMATION

Corresponding Author

*E-mail: rodriban@fisica.ufmg.br.

Notes

The authors declare no competing financial interest.

■ ACKNOWLEDGMENTS

We would like to thank the Brazilian National Light Synchrotron Laboratory, the Microscopy Center of Universidade Federal de Minas Gerais, the Brazilian agencies CNPq, CAPES, FAPEMIG, as well as the Portuguese agency FCT for the technical and financial support of this work. We would also like to thank the Prometeu cluster at the Physics Institute of Universidade Federal da Bahia used for the DFT calculations.

■ REFERENCES

(1) Duan, X.; Lieber, C. M. *Adv. Mater.* **2000**, *12*, 298−302.
(2) Poole, P. J.; Lefebvre, J.; Fraser, J. *Appl. Phys. Lett.* **2003**, *83*, 2055−2057.
(3) Lopez-Richard, V.; González, J. C.; Matinaga, F. M.; Trallero-Giner, C.; Ribeiro, E.; Rebello Sousa Dias, M.; Villegas-Lelovsky, L.; Marques, G. E. *Nano Lett.* **2009**, *9*, 3129−3136.
(4) González, J. C.; Malachias, A.; Andrade, R-Ribeiro; de Sousa, J. C.; Moreira, M. V. B.; de Oliveira, A. G. *J. Nanosci. Nanotechnol.* **2009**, *9*, 4673−4678.
(5) Dick, K. A.; Deppert, K.; Mårtensson, T.; Mandl, B.; Samuelson, L.; Seifert, W. *Nano Lett.* **2005**, *5*, 761−764.
(6) Dayeh, S. A.; Yu, E. T.; Wang, D. *Nano Lett.* **2007**, *7*, 2486−2490.
(7) Lim, S. K.; Tambe, M. J.; Brewster, M. M.; Gradeča, S. *Nano Lett.* **2008**, *8*, 1386−1392.
(8) González, J. C.; da Silva, M. I. N.; Lozano, X. S.; Zanchet, D.; Ugarte, D.; Ribeiro, E.; Gutiérrez, H. R.; Cotta, M. A. *J. Nanosci. Nanotechnol.* **2006**, *6*, 2182−2186.
(9) Falcão, B.; et al. *J. Mater. Sci.* **2012**, DOI: 10.1007/s10853-012-6941-x.
(10) Hiruma, K.; Murakoshi, H.; Yazawa, M.; Ogawa, K.; Fukuhara, S.; Shirai, M.; Katsuyama, T. *IEICE Trans. Electron.* **1994**, *E77-C*, 1420−1425.
(11) Mårtensson, T.; Wallenberg, L. R.; Samuelson, L.; et al. *Nano Lett.* **2004**, *4*, 1987−1990.
(12) Kim, Y.; Joyce, J. H.; Gao, Q.; Tan, H. H.; Jagadish, C.; Paladugu, M.; Zou, J.; Suvorova, A. A. *Nano Lett.* **2006**, *6*, 599−604.
(13) Dubrovskii, V. G.; Sibirev, N. V.; Cirlin, G. E.; Harmand, J. C.; Ustinov, V. M. *Phys. Rev. E* **2006**, *73*, 021603.1−10.
(14) Dubrovskii, V. G.; Sibirev, N. V.; Suris, R. A.; Cirlin, G. E.; Ustinov, V. M.; Tchernysheva, M.; Harmand, J. C. *Semiconductors* **2006**, *40*, 1075−1082.
(15) www.gel.usherbrooke.ca/casino
(16) Adachi, S.; *Physical Properties of III-Y Semiconductor Compounds*, John Wiley and Sons: New York, 1992.
(17) Wagner, R. S.; Ellis, W. C. *Appl. Phys. Lett.* **1964**, *4*, 89−90.
(18) Givargizov, E. I. *J. Cryst. Growth* **1975**, *31*, 20−30.
(19) Persson, A. I.; Larsson, M. W.; Stenström, S.; Ohlsson, B. J.; Samuelson, L.; Wallenberg, L. R. *Nat. Mater.* **2004**, *3*, 677−681.
(20) Bauer, J.; Gottschalch, V.; Wagner, G. *J. Appl. Phys.* **2008**, *104*, 114315.1−6.
(21) Hurle, D. T. J. *Handbook of Crystal Growth: Bulk Crystal Growth*; Elsevier North-Holland, 1994; *Vol. 2*;
(22) Kukushkin, S. A.; Osipov, A. V. *Prog. Surf. Sci.* **1996**, *51*, 1−107.
(23) López, M.; Nomura, Y. *J. Cryst. Growth* **1995**, *150*, 68−72.
(24) Nishinaga, T.; Shen, X. Q.; Kishimoto, D. *J. Cryst. Growth* **1996**, *163*, 60−66.
(25) Nomura, Y.; Morishita, Y.; Goto, S.; Katayama, Y.; Isu, T. *Appl. Phys. Lett.* **1994**, *64*, 1123−1125.
(26) Takebe, T.; Fujii, M.; Yamamoto, T.; Fujita, K.; Watanabe, T. *J. Appl. Phys.* **1997**, *81*, 7273−7281.
(27) Seifert, W.; et al. *J. Cryst. Growth* **2004**, *272*, 211−220.
(28) Mozume, T.; Ohbu, I. *Jpn. J. Appl. Phys.* **1992**, *31*, 3277−3281.
(29) Tersoff, J.; Johnson, M. D.; Orr, B. G. *Phys. Rev. Lett.* **1997**, *78*, 282−285.
(30) Kaxiras, E.; Bar-Yam, Y.; Joannopoulos, J. D.; Pandy, K. C. *Phys. Rev. B* **1987**, *35*, 9625−9635.
(31) Giannozzi, P.; et al. *J. Phys.: Condens. Matter* **2009**, *21*, 395502.1−19.
(32) The pseudopotentials used in the calculations are As.pbe-n-van.UPF and Ga.pbe-nsp-van.UPF from http://www.quantum-espresso.org
(33) Kaxiras, E.; Bar-Yam, Y.; Joannopoulos, J. D.; Pandey, K. C. *Phys. Rev. B* **1986**, *33*, 4406−4409.